

CP Violation and Matter Effect in Long Baseline Neutrino Oscillation Experiments

Jiro Arafune*, Masafumi Koike† and Joe Sato‡

Institute for Cosmic Ray Research, University of Tokyo, Midori-cho, Tanashi, Tokyo 188, Japan

Abstract

We show simple methods how to separate pure CP violating effect from matter effect in long baseline neutrino oscillation experiments with three generations of neutrinos. We give compact formulae for neutrino oscillation probabilities assuming one of the three neutrino masses (presumably ν_τ mass) to be much larger than the other masses and the effective mass due to matter effect. Two methods are shown: One is to observe envelopes of the curves of oscillation probabilities as functions of neutrino energy; a merit of this method is that only a single detector is enough to determine the presence of CP violation. The other is to compare experiments with at least two different baseline lengths; this has a merit that it needs only narrow energy range of oscillation data.

1 Introduction

The CP violation has been observed only in the hadron sector, and it is very hard for us to understand where the CP violation originates from. If we observe CP violation in the lepton sector through the neutrino oscillation experiments, we will be given an invaluable key to study the origin of CP violation and to go beyond the Standard Model.

The neutrino oscillation search is a powerful experiment which can examine masses and/or mixing angles of the neutrinos. The several underground experiments, in fact, have shown lack of the solar neutrinos [1, 2, 3, 4] and anomaly in the atmospheric neutrinos [5, 6, 7]¹, strongly indicating the neutrino oscillation [10, 11, 12]. The solar neutrino deficit implies a mass difference of $10^{-5} \sim 10^{-4} \text{eV}^2$, while the atmospheric neutrino anomaly suggests a mass difference around $10^{-3} \sim 10^{-2} \text{eV}^2$ [10, 11, 12].

The latter encourages us to make long baseline neutrino oscillation experiments. Recently such experiments are planned and will be operated in the near future [13, 14]. It

*e-mail address: arafune@icrr.u-tokyo.ac.jp

†e-mail address: koike@icrr.u-tokyo.ac.jp

‡e-mail address: joe@icrr.u-tokyo.ac.jp

¹Some experiments have not observed the atmospheric neutrino anomaly [8, 9].

is now desirable to examine whether there is a chance to observe not only the neutrino oscillation but also the CP or T violation by long baseline experiments [15, 16]. Two of the present authors have studied how large T violation we may be seen in long baseline experiments [16], but they have not answered the question how the CP violation is distinguished from the matter effect, in case both the solar neutrino deficit and the atmospheric neutrino anomaly are attributed to the neutrino oscillation (In this case the matter effect is expected to give a fake CP-violation effect comparable to pure CP-violation effect).

In this paper we will answer this question. In sec. 2 we briefly review neutrino oscillation for 3 generations, and give very compact formulae describing neutrino oscillation in the presence of matter (The detailed derivation of the formulae is given in the Appendix). In sec. 3 we show two methods to distinguish pure CP violation from matter effect. In sec. 4 we summarize our work and give discussions.

2 Compact Formulae for the Neutrino Oscillation Probabilities

2.1 Brief Review and Parameterization

Let us briefly review CP violation in neutrino oscillation [17, 18, 19] to clarify our notation.

We assume three generations of neutrinos which have mass eigenvalues $m_i (i = 1, 2, 3)$ and mixing matrix $U^{(0)}$ relating the flavor eigenstates $\nu_\alpha (\alpha = e, \mu, \tau)$ and the mass eigenstates in the vacuum $\nu'_i (i = 1, 2, 3)$ as

$$\nu_\alpha = U_{\alpha i}^{(0)} \nu'_i. \quad (1)$$

We parametrize $U^{(0)}$ [20, 21, 22] with the Gell-Mann matrices λ_i 's as

$$\begin{aligned} U^{(0)} &= e^{i\psi\lambda_7} \Gamma e^{i\phi\lambda_5} e^{i\omega\lambda_2} \\ &= \begin{pmatrix} 1 & 0 & 0 \\ 0 & c_\psi & s_\psi \\ 0 & -s_\psi & c_\psi \end{pmatrix} \begin{pmatrix} 1 & 0 & 0 \\ 0 & 1 & 0 \\ 0 & 0 & e^{i\delta} \end{pmatrix} \begin{pmatrix} c_\phi & 0 & s_\phi \\ 0 & 1 & 0 \\ -s_\phi & 0 & c_\phi \end{pmatrix} \begin{pmatrix} c_\omega & s_\omega & 0 \\ -s_\omega & c_\omega & 0 \\ 0 & 0 & 1 \end{pmatrix} \\ &= \begin{pmatrix} c_\phi c_\omega & c_\phi s_\omega & s_\phi \\ -c_\psi s_\omega - s_\psi s_\phi c_\omega e^{i\delta} & c_\psi c_\omega - s_\psi s_\phi s_\omega e^{i\delta} & s_\psi c_\phi e^{i\delta} \\ s_\psi s_\omega - c_\psi s_\phi c_\omega e^{i\delta} & -s_\psi c_\omega - c_\psi s_\phi s_\omega e^{i\delta} & c_\psi c_\phi e^{i\delta} \end{pmatrix}, \end{aligned} \quad (2)$$

where $c_\psi = \cos \psi$, $s_\phi = \sin \phi$, etc.

The evolution equation for the flavor eigenstate vector in the vacuum is

$$\begin{aligned} i \frac{d\nu}{dx} &= -U^{(0)} \text{diag}(p_1, p_2, p_3) U^{(0)\dagger} \nu \\ &\simeq \left\{ -p_1 + \frac{1}{2E} U^{(0)} \text{diag}(0, \delta m_{21}^2, \delta m_{31}^2) U^{(0)\dagger} \right\} \nu, \end{aligned} \quad (3)$$

where p_i 's are the momenta, E is the energy and $\delta m_{ij}^2 = m_i^2 - m_j^2$. Neglecting the term p_1 which gives an irrelevant overall phase, we have

$$i\frac{d\nu}{dx} = \frac{1}{2E}U^{(0)}\text{diag}(0, \delta m_{21}^2, \delta m_{31}^2)U^{(0)\dagger}\nu. \quad (4)$$

Similarly the evolution equation in matter is expressed as

$$i\frac{d\nu}{dx} = H\nu, \quad (5)$$

where

$$H \equiv \frac{1}{2E}U\text{diag}(\mu_1^2, \mu_2^2, \mu_3^2)U^\dagger, \quad (6)$$

with a unitary mixing matrix U and the effective mass squared μ_i^2 's ($i = 1, 2, 3$). The matrix U and the masses μ_i 's are determined by

$$U \begin{pmatrix} \mu_1^2 & 0 & 0 \\ 0 & \mu_2^2 & 0 \\ 0 & 0 & \mu_3^2 \end{pmatrix} U^\dagger = U^{(0)} \begin{pmatrix} 0 & 0 & 0 \\ 0 & \delta m_{21}^2 & 0 \\ 0 & 0 & \delta m_{31}^2 \end{pmatrix} U^{(0)\dagger} + \begin{pmatrix} a & 0 & 0 \\ 0 & 0 & 0 \\ 0 & 0 & 0 \end{pmatrix}. \quad (7)$$

Here

$$\begin{aligned} a &\equiv 2\sqrt{2}G_{\text{F}}n_e E \\ &= 7.56 \times 10^{-5} \text{eV}^2 \frac{\rho}{\text{g cm}^{-3}} \frac{E}{\text{GeV}}, \end{aligned} \quad (8)$$

where n_e is the electron density and ρ is the matter density. The solution of eq.(5) is then

$$\nu(x) = S(x)\nu(0) \quad (9)$$

with

$$S \equiv \text{T} e^{-i\int_0^x ds H(s)} \quad (10)$$

(T being the symbol for time ordering), giving the oscillation probability for $\nu_\alpha \rightarrow \nu_\beta$ ($\alpha, \beta = e, \mu, \tau$) at distance L as

$$P(\nu_\alpha \rightarrow \nu_\beta; L) = |S_{\beta\alpha}(L)|^2. \quad (11)$$

The oscillation probability for the antineutrinos $P(\bar{\nu}_\alpha \rightarrow \bar{\nu}_\beta)$ is obtained by replacing $a \rightarrow -a$ and $U \rightarrow U^*$ (i.e. $\delta \rightarrow -\delta$) in eq.(11).

We assume in the following the matter density is independent of space and time for simplicity, and have

$$S(x) = e^{-iHx}. \quad (12)$$

2.2 Approximation of the Oscillation Probability

If we attribute both the solar neutrino deficit and the atmospheric neutrino anomaly to the neutrino oscillation with MSW solution for the solar neutrinos, we find most plausible solutions to satisfy $\delta m_{21}^2 \ll \delta m_{31}^2$ and $a \ll \delta m_{31}^2$ [10, 11]. In the following we assume $a, \delta m_{21}^2 \ll \delta m_{31}^2$ ². This case is also interesting when we consider the long baseline neutrino oscillation experiments to be done in the near future [13, 14].

Decomposing $H = H_0 + H_1$ with

$$H_0 = \frac{1}{2E} U^{(0)} \begin{pmatrix} 0 & & \\ & 0 & \\ & & \delta m_{31}^2 \end{pmatrix} U^{(0)\dagger} \quad (13)$$

and

$$H_1 = \frac{1}{2E} \left\{ U^{(0)} \begin{pmatrix} 0 & & \\ & \delta m_{21}^2 & \\ & & 0 \end{pmatrix} U^{(0)\dagger} + \begin{pmatrix} a & & \\ & 0 & \\ & & 0 \end{pmatrix} \right\}, \quad (14)$$

we treat H_1 as a perturbation and calculate eq.(12) up to the first order in a and δm_{21}^2 . Defining $\Omega(x)$ and $H_1(x)$ as

$$\Omega(x) = e^{iH_0 x} S(x) \quad (15)$$

and

$$H_1(x) = e^{iH_0 x} H_1 e^{-iH_0 x}, \quad (16)$$

we have

$$i \frac{d\Omega}{dx} = H_1(x) \Omega(x) \quad (17)$$

and

$$\Omega(0) = 1, \quad (18)$$

which give the solution³

$$\begin{aligned} \Omega(x) &= \text{T} e^{-i \int_0^x ds H_1(s)} \\ &\simeq 1 - i \int_0^x ds H_1(s). \end{aligned} \quad (19)$$

We note the approximation (19) requires

$$\frac{ax}{2E} \ll 1 \quad \text{and} \quad \frac{\delta m_{21}^2 x}{2E} \ll 1. \quad (20)$$

The equations (15) and (19) give

$$S(x) \simeq e^{-iH_0 x} + e^{-iH_0 x} (-i) \int_0^x ds H_1(s). \quad (21)$$

²For the case $\delta m_{21}^2 \ll a \ll \delta m_{31}^2$ see ref.[16].

³We note the eq.(19) is correct for a case where the matter density depends on x .

We then obtain the oscillation probabilities $P(\nu_\mu \rightarrow \nu_e)$, $P(\nu_\mu \rightarrow \nu_\mu)$ and $P(\nu_\mu \rightarrow \nu_\tau)$ in the lowest order approximation as

$$\begin{aligned}
P(\nu_\mu \rightarrow \nu_e; L) &= 4 \sin^2 \frac{\delta m_{31}^2 L}{4E} c_\phi^2 s_\phi^2 s_\psi^2 \left\{ 1 + \frac{a}{\delta m_{31}^2} \cdot 2(1 - 2s_\phi^2) \right\} \\
&+ 2 \frac{\delta m_{31}^2 L}{2E} \sin \frac{\delta m_{31}^2 L}{2E} c_\phi^2 s_\phi s_\psi \left\{ -\frac{a}{\delta m_{31}^2} s_\phi s_\psi (1 - 2s_\phi^2) + \frac{\delta m_{21}^2}{\delta m_{31}^2} s_\omega (-s_\phi s_\psi s_\omega + c_\delta c_\psi c_\omega) \right\} \\
&- 4 \frac{\delta m_{21}^2 L}{2E} \sin^2 \frac{\delta m_{31}^2 L}{4E} s_\delta c_\phi^2 s_\phi c_\psi s_\psi c_\omega s_\omega, \tag{22}
\end{aligned}$$

$$\begin{aligned}
P(\nu_\mu \rightarrow \nu_\mu) &= 1 + 4 \sin^2 \frac{\delta m_{31}^2 L}{4E} c_\phi^2 s_\psi^2 \left\{ (c_\phi^2 s_\psi^2 - 1) + \frac{a}{\delta m_{31}^2} \cdot 2s_\phi^2 (1 - 2c_\phi^2 s_\psi^2) \right\} \\
&+ 2 \frac{\delta m_{31}^2 L}{2E} \sin \frac{L \delta m_{31}^2}{2E} c_\phi^2 s_\psi^2 \left\{ \frac{a}{\delta m_{31}^2} s_\phi^2 (2c_\phi^2 s_\psi^2 - 1) \right. \\
&\left. + \frac{\delta m_{21}^2}{\delta m_{31}^2} (s_\phi^2 s_\psi^2 s_\omega^2 + c_\omega^2 c_\psi^2 - 2c_\delta c_\psi c_\omega s_\phi s_\psi s_\omega) \right\} \tag{23}
\end{aligned}$$

and

$$\begin{aligned}
P(\nu_\mu \rightarrow \nu_\tau) &= 4 \sin^2 \frac{\delta m_{31}^2 L}{4E} c_\phi^4 c_\psi^2 s_\psi^2 \left(1 - \frac{a}{\delta m_{31}^2} \cdot 4s_\phi^2 \right) \\
&+ 2 \frac{\delta m_{31}^2 L}{2E} \sin \frac{\delta m_{31}^2 L}{2E} c_\phi^2 c_\psi s_\psi \left[\frac{a}{\delta m_{31}^2} 2c_\phi^2 c_\psi s_\phi^2 s_\psi \right. \\
&\left. - \frac{\delta m_{21}^2}{\delta m_{31}^2} \left\{ (c_\omega^2 - s_\omega^2 s_\phi^2) c_\psi s_\psi + c_\delta (c_\psi^2 - s_\psi^2) s_\phi c_\omega s_\omega \right\} \right] \\
&+ 4 \frac{\delta m_{21}^2 L}{2E} \sin^2 \frac{\delta m_{31}^2 L}{4E} s_\delta c_\phi^2 s_\phi c_\psi s_\psi c_\omega s_\omega. \tag{24}
\end{aligned}$$

(Detailed derivation is presented in the Appendix). Recalling that $P(\bar{\nu}_\alpha \rightarrow \bar{\nu}_\beta)$ is obtained from $P(\nu_\alpha \rightarrow \nu_\beta)$ by the replacements $a \rightarrow -a$ and $\delta \rightarrow -\delta$, we have

$$\begin{aligned}
\Delta P(\nu_\mu \rightarrow \nu_e) &\equiv P(\nu_\mu \rightarrow \nu_e; L) - P(\bar{\nu}_\mu \rightarrow \bar{\nu}_e; L) \\
&= \Delta P_1(\nu_\mu \rightarrow \nu_e) + \Delta P_2(\nu_\mu \rightarrow \nu_e) + \Delta P_3(\nu_\mu \rightarrow \nu_e) \tag{25}
\end{aligned}$$

with

$$\Delta P_1(\nu_\mu \rightarrow \nu_e) = 16 \frac{a}{\delta m_{31}^2} \sin^2 \frac{\delta m_{31}^2 L}{4E} c_\phi^2 s_\phi^2 s_\psi^2 (1 - 2s_\phi^2), \tag{26}$$

$$\Delta P_2(\nu_\mu \rightarrow \nu_e) = -4 \frac{aL}{2E} \sin \frac{\delta m_{31}^2 L}{2E} c_\phi^2 s_\phi^2 s_\psi^2 (1 - 2s_\phi^2), \tag{27}$$

and

$$\Delta P_3(\nu_\mu \rightarrow \nu_e) = -8 \frac{\delta m_{21}^2 L}{2E} \sin^2 \frac{\delta m_{31}^2 L}{4E} s_\delta c_\phi^2 s_\phi c_\psi s_\psi c_\omega s_\omega. \tag{28}$$

Similarly we obtain

$$\begin{aligned} & \Delta P(\nu_\mu \rightarrow \nu_\mu) \\ = & 16 \frac{a}{\delta m_{31}^2} \left[\sin^2 \frac{\delta m_{31}^2 L}{4E} - \frac{1}{4} \frac{\delta m_{31}^2 L}{2E} \sin \frac{\delta m_{31}^2 L}{2E} \right] c_\phi^2 s_\phi^2 s_\psi^2 (1 - 2c_\phi^2 s_\psi^2) \end{aligned} \quad (29)$$

and

$$\begin{aligned} & \Delta P(\nu_\mu \rightarrow \nu_\tau) \\ = & -32 \frac{a}{\delta m_{31}^2} \left[\sin^2 \frac{\delta m_{31}^2 L}{4E} - \frac{1}{4} \frac{\delta m_{31}^2 L}{2E} \sin \frac{\delta m_{31}^2 L}{2E} \right] c_\phi^4 s_\phi^2 c_\psi^2 s_\psi^2 \\ & + 8 \frac{\delta m_{21}^2 L}{2E} \sin^2 \frac{\delta m_{31}^2 L}{4E} s_\delta c_\phi^2 s_\phi c_\psi s_\psi c_\omega s_\omega. \end{aligned} \quad (30)$$

Here we make some comments.

1. $P(\nu_\alpha \rightarrow \nu_\beta)$'s and $\Delta P(\nu_\alpha \rightarrow \nu_\beta)$'s depend on L and E as functions of L/E apart from the matter effect factor $a (= 2\sqrt{2}G_F n_e E)$.
2. At least four experimental data are necessary to determine the function $\Delta P(\nu_\mu \rightarrow \nu_e)$, since it has four unknown factors: δm_{31}^2 , δm_{21}^2 , $c_\phi^2 s_\phi^2 s_\psi^2 (1 - 2s_\phi^2)$ and $s_\delta c_\phi^2 s_\phi c_\psi s_\psi c_\omega s_\omega$. In order to determine all the mixing angles and the CP violating phase, we need to observe $P(\nu_\mu \rightarrow \nu_\mu)$ and $P(\bar{\nu}_\mu \rightarrow \bar{\nu}_\mu)$ in addition.
3. $\Delta P(\nu_\mu \rightarrow \nu_\mu)$ is independent of δ and consists only of matter effect term.

3 Separation of Pure CP Violating Effect from the Matter Effect

Next we investigate how we can divide $\Delta P(\nu_\mu \rightarrow \nu_e)$ into a pure CP-violation part and a matter effect part⁴. The terms $\Delta P_1(\nu_\mu \rightarrow \nu_e)$ and $\Delta P_2(\nu_\mu \rightarrow \nu_e)$, which are proportional to “ a ”, are due to effect of the matter along the path. The term $\Delta P_3(\nu_\mu \rightarrow \nu_e)$, which is proportional to s_δ , is due to the pure CP violation (We simply call $\Delta P_i(\nu_\mu \rightarrow \nu_e)$ as ΔP_i hereafter). In the following we introduce two methods to separate the pure CP violating effect ΔP_3 from the matter effect $\Delta P_1 + \Delta P_2$.

3.1 Observation of Envelope Patterns

One method is to observe the pattern of the envelope of ΔP , and to separate ΔP_3 from it. Considering the energy dependence of $a(\propto E)$, we see that $\Delta P_1/L$, $\Delta P_2/L$ and ΔP_3 depend on a variable L/E alone. The dependences of them on the variable L/E , however,

⁴It is straightforward to extend the following arguments to other processes like $\nu_\mu \rightarrow \nu_\tau$. We present the cases of $\nu_\mu \rightarrow \nu_e$ and $\bar{\nu}_\mu \rightarrow \bar{\nu}_e$ as examples.

are different from each other as seen in Fig. 1. Each of them oscillates with common zeros at $L/E = 2\pi n/\delta m_{31}^2$ ($n = 0, 1, 2, \dots$) and has its characteristic envelope. The envelope of $\Delta P_1/L$ decreases monotonously. That of $\Delta P_2/L$ is flat. That of ΔP_3 increases linearly. It is thus possible to separate these three functions and determine CP violating effect ΔP_3 by measuring the probability ΔP over wide energy range in the long baseline neutrino oscillation experiments. This method has a merit that we can determine the pure CP violating effect with a single detector.

In Fig. 2 we give the probabilities $P(\nu_\mu \rightarrow \nu_e)$ and $P(\bar{\nu}_\mu \rightarrow \bar{\nu}_e)$ for a set of typical parameters which are consistent with the solar and atmospheric neutrino experiments [11]: $\delta m_{21}^2 = 10^{-4} \text{ eV}^2$, $\delta m_{31}^2 = 10^{-2} \text{ eV}^2$, $s_\psi = 1/\sqrt{2}$, $s_\phi = \sqrt{0.1}$ and $s_\omega = 1/2$. We see the effect of pure CP violation in Fig. 2(a), since we find that the curve ΔP has the envelope characteristic of ΔP_3 . We show in Fig. 3 the same probabilities as Fig. 2(a) but as functions of E to see the energy dependence more directly.

We comment that the envelope behavior of ΔP can be understood rather simply as follows: The term ΔP_3 is proportional to [23, 16]

$$\begin{aligned} f &= \sin \Delta_{21} + \sin \Delta_{32} + \sin \Delta_{13} \\ &= -4 \sin \frac{\Delta_{21}}{2} \sin \frac{\Delta_{32}}{2} \sin \frac{\Delta_{13}}{2}, \end{aligned} \quad (31)$$

where

$$\Delta_{ij} = \frac{\delta \mu_{ij}^2 L}{2E}. \quad (32)$$

Since we are interested in the first several peaks of f , we have

$$\Delta_{31}, \Delta_{32} \sim \mathcal{O}(1). \quad (33)$$

On the other hand we have

$$\Delta_{21} \ll 1, \quad (34)$$

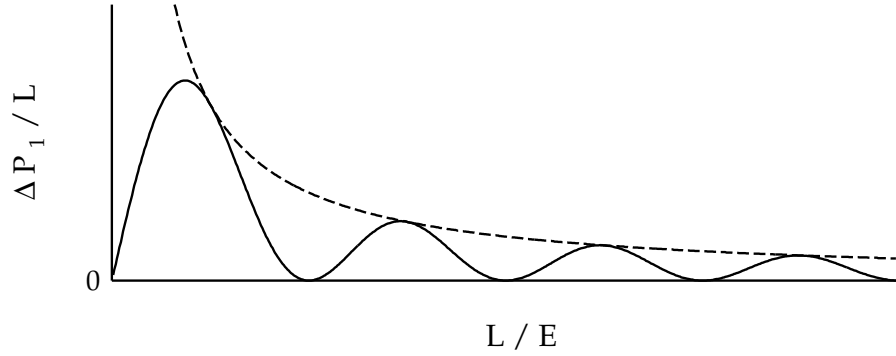
because $\Delta_{21} \ll \Delta_{31}, \Delta_{32}$. Taking into account

$$\Delta_{21} + \Delta_{32} + \Delta_{13} = 0 \quad (35)$$

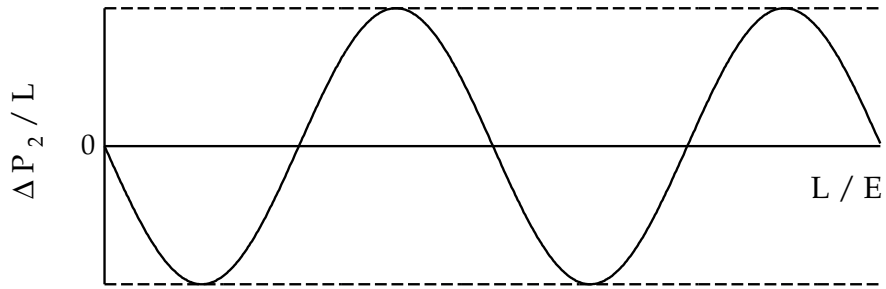
and eqs. (33) and (34), we obtain

$$\Delta P_3 \propto f \simeq 2\Delta_{21} \sin^2 \frac{\Delta_{31}}{2}. \quad (36)$$

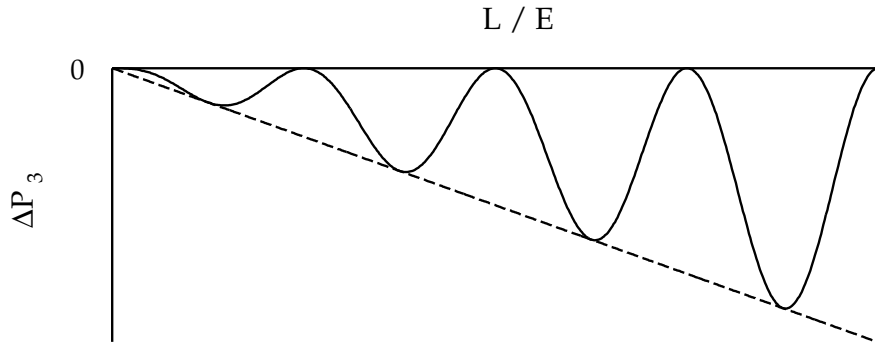
This shows ΔP_3 has a linearly increasing envelope $\Delta_{21} \propto L/E$. On the other hand, the envelopes of ΔP_1 and ΔP_2 do not increase with L/E for fixed L , and it makes ΔP_3 dominant in ΔP for large L/E .



(a) Matter effect term $\Delta P_1(\nu_\mu \rightarrow \nu_e)$ divided by L for $c_\phi^2 s_\phi^2 s_\psi^2 (1 - 2s_\phi^2) > 0$. The envelope decreases monotonously with L/E .

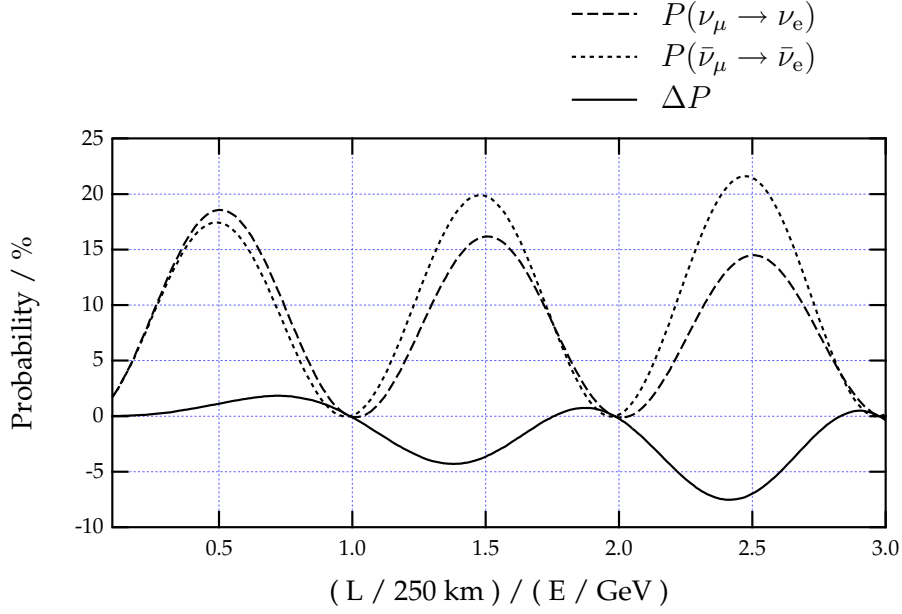


(b) Matter effect term $\Delta P_2(\nu_\mu \rightarrow \nu_e)$ divided by L for $c_\phi^2 s_\phi^2 s_\psi^2 (1 - 2s_\phi^2) > 0$. The envelope is flat.

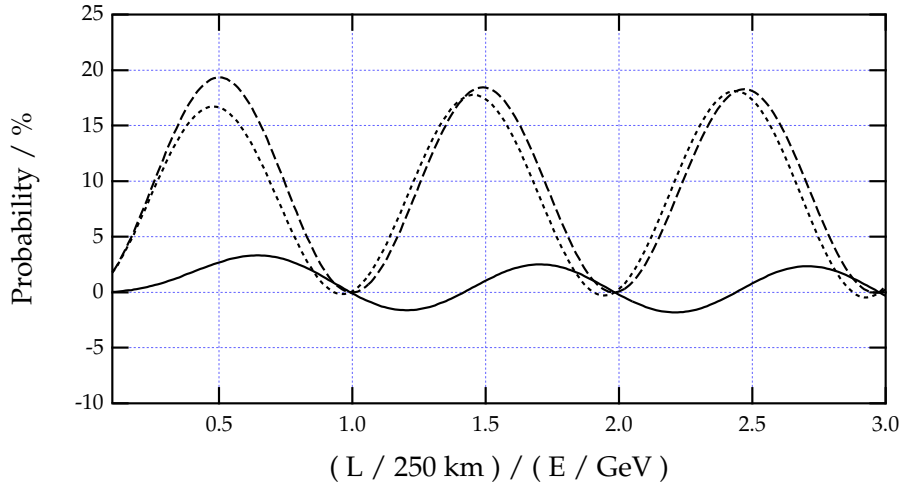


(c) CP-violation effect term $\Delta P_3(\nu_\mu \rightarrow \nu_e)$ for $s_\delta c_\phi^2 s_\phi c_\psi s_\psi c_\omega s_\omega > 0$. The envelope increases linearly with L/E .

Figure 1: The oscillation behaviors of the $\Delta P_1, \Delta P_2$ and ΔP_3 .



(a) The oscillation probabilities as functions of L/E for $\delta = \pi/2$.



(b) The oscillation probabilities as functions of L/E for $\delta = 0$.

Figure 2: The oscillation probabilities for $\delta = \pi/2$ (Fig. 2(a)) and $\delta = 0$ (Fig. 2(b)). $P(\nu_\mu \rightarrow \nu_e)$, $P(\bar{\nu}_\mu \rightarrow \bar{\nu}_e)$ and $\Delta P(\nu_\mu \rightarrow \nu_e)$ are given by a broken line, a dotted line and a solid line, respectively. Here $\rho = 3\text{g cm}^{-3}$ and $L = 250\text{ km}$ (the distance between KEK and Super-Kamiokande) are taken. Other parameters are fixed at the following values which are consistent with the solar and atmospheric neutrino experiments [11]: $\delta m_{21}^2 = 10^{-4}\text{ eV}^2$, $\delta m_{31}^2 = 10^{-2}\text{ eV}^2$, $s_\psi = 1/\sqrt{2}$, $s_\phi = \sqrt{0.1}$ and $s_\omega = 1/2$.

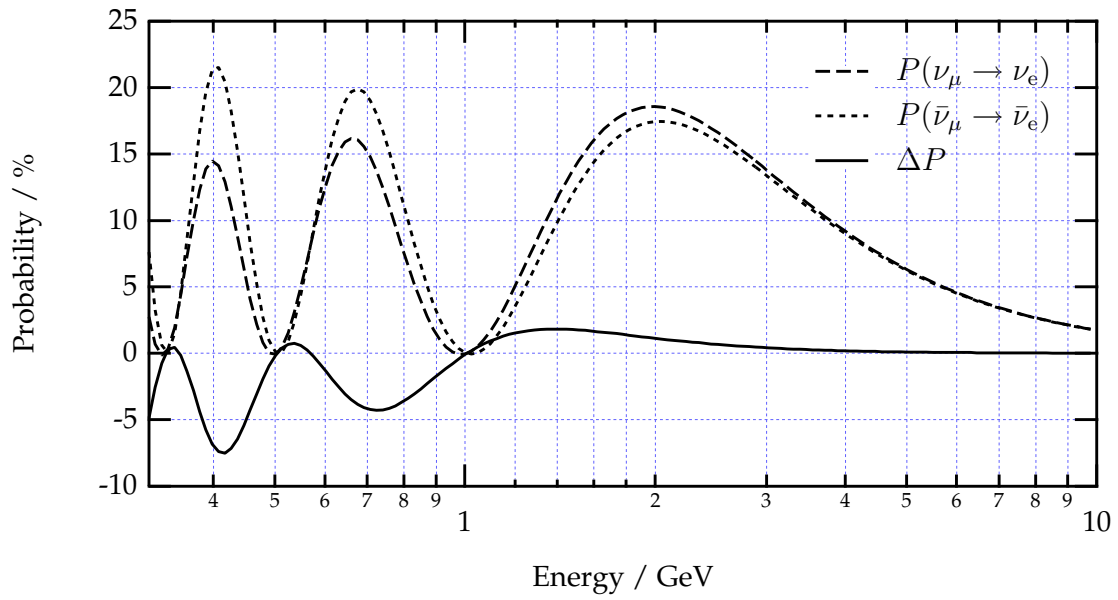


Figure 3: The oscillation probabilities as functions of E . Parameters are taken the same as in Fig. 2(a).

3.2 Comparison of Experiments with Different L 's

The other method is to separate the pure CP violating effect by comparison of experiments with two different L 's. Suppose that two experiments, one with $L = L_1$ and the other $L = L_2$, are available. We observe two probabilities $P(\nu_\mu \rightarrow \nu_e; L_1)$ at energy E_1 and $P(\nu_\mu \rightarrow \nu_e; L_2)$ at energy E_2 with $L_1/E_1 = L_2/E_2$. Recalling that $P(\nu_\mu \rightarrow \nu_e; L)$ is a function of L/E apart from the matter effect factor $a(\propto E)$, we see that the difference

$$\{P(\nu_\mu \rightarrow \nu_e; L_1) - P(\nu_\mu \rightarrow \nu_e; L_2)\}_{L_1/E_1=L_2/E_2} \quad (37)$$

is due only to terms proportional to “ a ”. We obtain ΔP_3 by subtracting these terms ($\Delta P_1 + \Delta P_2$) from $\Delta P(\nu_\mu \rightarrow \nu_e)$ as⁵

$$\begin{aligned} & \Delta P_3(\nu_\mu \rightarrow \nu_e; L_1) \\ = & \left[\Delta P(\nu_\mu \rightarrow \nu_e; L_1) - \frac{2L_1}{L_2 - L_1} \{P(\nu_\mu \rightarrow \nu_e; L_2) - P(\nu_\mu \rightarrow \nu_e; L_1)\} \right]_{L/E=\text{const.}} \quad (38) \end{aligned}$$

$$= \left[\Delta P(\nu_\mu \rightarrow \nu_e; L_1) - \frac{L_1}{L_2 - L_1} \{\Delta P(\nu_\mu \rightarrow \nu_e; L_2) - \Delta P(\nu_\mu \rightarrow \nu_e; L_1)\} \right]_{L/E=\text{const.}} \quad (39)$$

This method has a merit that it does not need to observe the envelope nor many oscillation bumps in the low energy range.

In Fig. 4 we compare $P(\nu_\mu \rightarrow \nu_e)$ for $L = 250\text{km}$ (KEK/Super-Kamiokande experiment) with that for $L = 730\text{km}$ (Minos experiment) in a case with the same neutrino masses and mixing angles as those in Fig. 2(a) (or Fig. 3). We see their difference, consisting only of the matter effect, has the same shape as the solid line in Fig. 2(b) up to a overall constant. We also show the pure CP violating effect obtained by the two probabilities with eq.(38). This curve has a linearly increasing envelope as seen in Fig. 1(c).

4 Summary and Discussions

We have given very simple formulae for the transition probabilities of neutrinos in long baseline experiments. They have taken into account not only the CP-violation effect but also the matter effect, and are applicable to such interesting parameter regions that can explain both the atmospheric neutrino anomaly and the solar neutrino deficit by the neutrino oscillation.

We have shown with the aid of these formulae two methods to distinguish pure CP violation from matter effect. The dependence of pure CP-violation effect on the energy E and the distance L is different from that of matter effect: The former depends on L/E alone and has a form $f(L/E)$, while the latter has a form $L \times g(L/E) \equiv E \times \tilde{g}(L/E)$. One method to distinguish is to observe closely the energy dependence of the difference $P(\nu_\mu \rightarrow \nu_e; L) - P(\bar{\nu}_\mu \rightarrow \bar{\nu}_e; L)$ including the envelope of oscillation bumps. The other is

⁵Note that the eq.(38) does not require $P(\bar{\nu}_\mu \rightarrow \bar{\nu}_e; L_2)$.

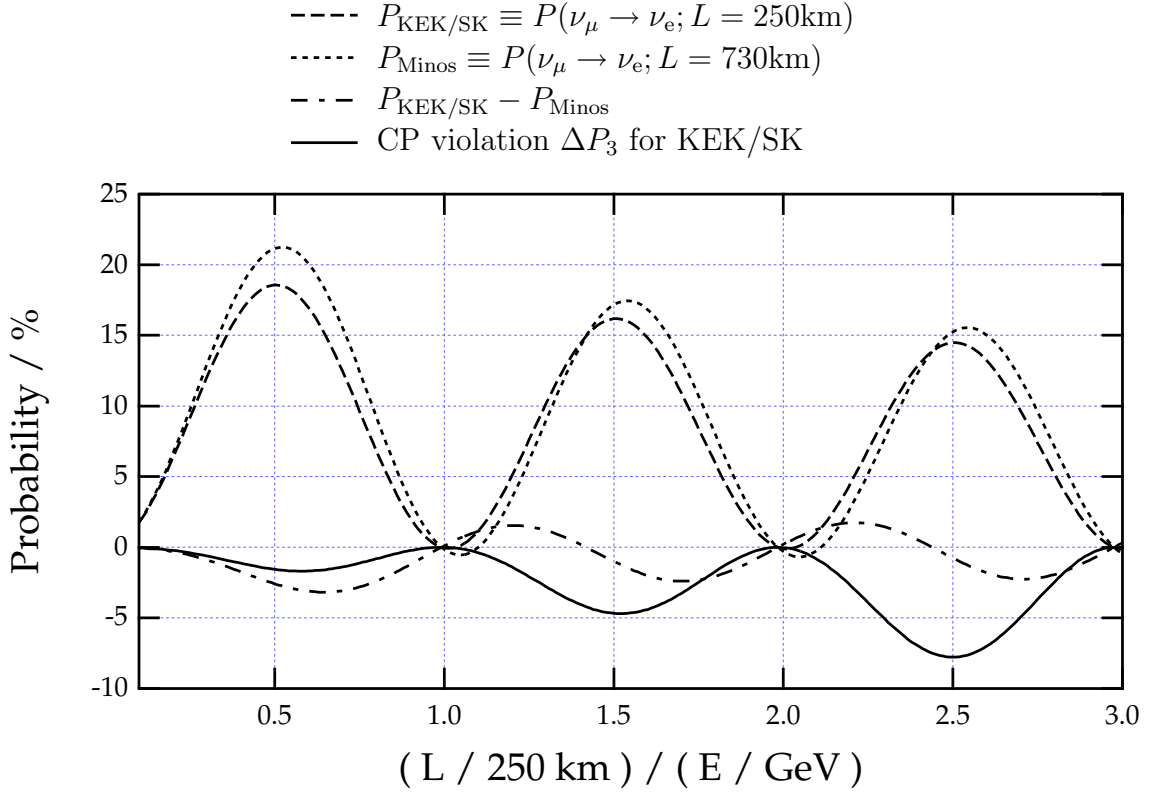


Figure 4: The oscillation probabilities $P(\nu_\mu \rightarrow \nu_e)$'s for KEK/Super-Kamiokande experiment with $L = 250\text{km}$ (broken line) and those for Minos experiment with $L = 730\text{km}$ (dotted line). Masses and mixing angles are the same as in Fig. 2(a). Their difference, which consists only of matter effect, is shown by a dot-dashed line. The pure CP violating effect in KEK/Super-Kamiokande experiment determined by eq.(38) is drawn by a solid line.

to compare results from two different distances L_1 and L_2 with $L_1/E_1 = L_2/E_2$ and then to subtract the matter effect by eq.(38) or eq.(39).

Each method has both its merits and demerits. The first one has a merit that we need experiments with only a single detector. A merit of the second is that we do not need wide range of energy (many bumps) to survey the neutrino oscillation.

It is desirable to make long baseline neutrino oscillation experiments with high intensity neutrino flux, and to study CP violation in the lepton sector experimentally.

A Derivation of the Oscillation Probabilities

Here we present the derivation of eq.(22) \sim eq.(24) with use of eq.(21), and show how well this approximation works. Let us set $S(x) = S_0(x) + S_1(x)$, defining

$$S_0(x) = e^{-iH_0x}, \quad (40)$$

$$S_1(x) = e^{-iH_0x}(-i) \int_0^x ds H_1(s). \quad (41)$$

We see

$$\begin{aligned} S_0(x)_{\beta\alpha} &= \left\{ U^{(0)} e^{-i\frac{x}{2E} \text{diag}(0,0,\delta m_{31}^2)} U^{(0)\dagger} \right\}_{\beta\alpha} \\ &= \delta_{\beta\alpha} + U_{\beta 3}^{(0)} U_{\alpha 3}^{(0)*} \left(e^{-i\frac{\delta m_{31}^2 x}{2E}} - 1 \right) \end{aligned} \quad (42)$$

and

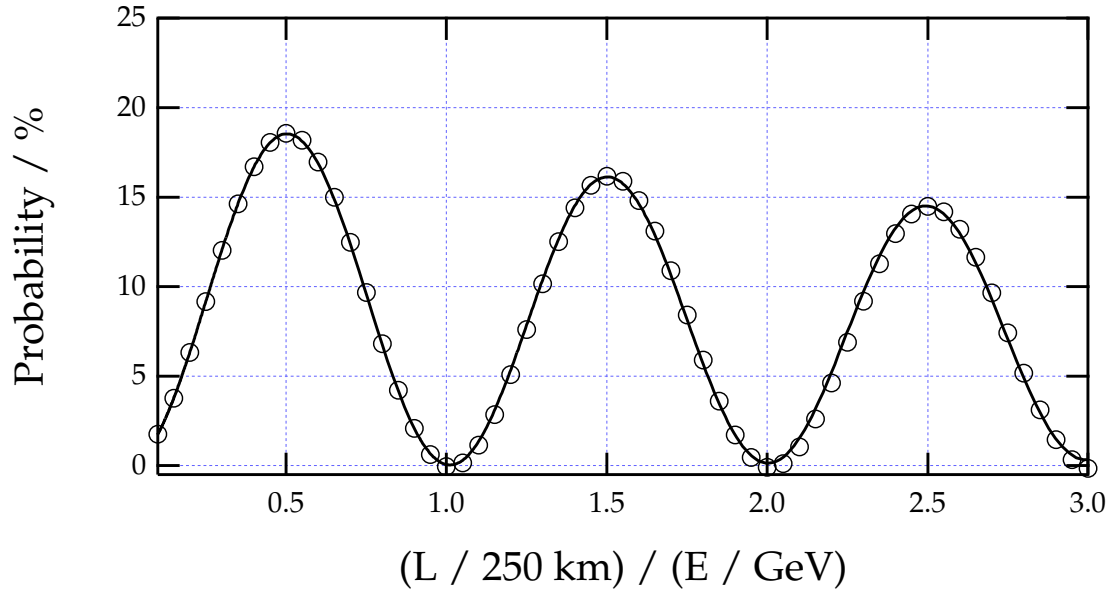
$$\begin{aligned} S_1(x)_{\beta\alpha} &= -i \int_0^x ds \left[e^{-iH_0(x-s)} H_1 e^{-iH_0s} \right]_{\beta\alpha} \\ &= -i U_{\beta i}^{(0)} U_{\gamma i}^{(0)*} (H_1)_{\gamma\delta} U_{\delta j}^{(0)} U_{\alpha j}^{(0)*} \Gamma(x)_{ij}, \end{aligned} \quad (43)$$

where

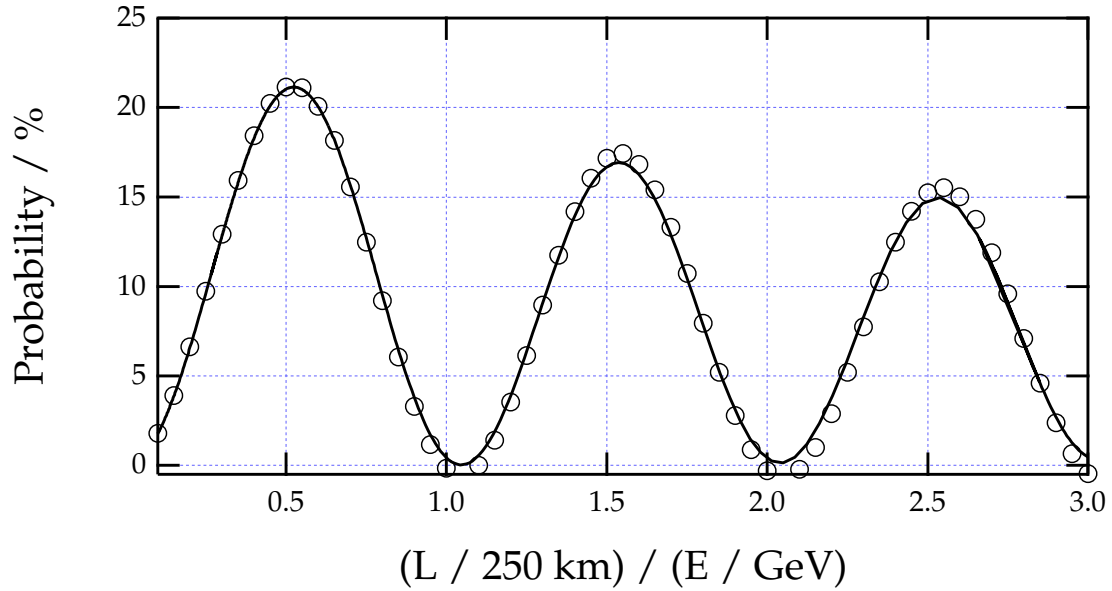
$$\begin{aligned} \Gamma(x)_{ij} &\equiv \int_0^x ds e^{-i\frac{\delta m_{31}^2}{2E} \{(x-s)\delta_{i3} + s\delta_{j3}\}} \\ &= \delta_{i3}\delta_{j3} \cdot x e^{-i\frac{\delta m_{31}^2 x}{2E}} \\ &+ \{(1 - \delta_{i3})\delta_{j3} + \delta_{i3}(1 - \delta_{j3})\} \cdot \left(-i\frac{\delta m_{31}^2}{2E} \right)^{-1} \left(e^{-i\frac{\delta m_{31}^2 x}{2E}} - 1 \right) \\ &+ (1 - \delta_{i3})(1 - \delta_{j3}) \cdot x. \end{aligned} \quad (44)$$

Using

$$\begin{aligned} U_{\gamma i}^{(0)*} (H_1)_{\gamma\delta} U_{\delta j}^{(0)} &= \frac{1}{2E} \left\{ \text{diag}(0, \delta m_{21}^2, 0) + U^{(0)\dagger} \text{diag}(a, 0, 0) U^{(0)} \right\}_{ij} \\ &= \frac{\delta m_{21}^2}{2E} \delta_{i2}\delta_{j2} + \frac{a}{2E} U_{1i}^{(0)*} U_{1j}^{(0)} \end{aligned} \quad (45)$$



(a) Exact and approximated values of $P(\nu_\mu \rightarrow \nu_e)$ for $L = 250$ km.



(b) Exact and approximated values of $P(\nu_\mu \rightarrow \nu_e)$ for $L = 730$ km.

Figure 5: Exact and approximated values of $P(\nu_\mu \rightarrow \nu_e)$ for $L = 250$ km (Fig. 5(a)) and those for $L = 730$ km (Fig. 5(b)). Exact values and approximated ones are shown by solid lines and white circles, respectively. The parameters $s_\psi, s_\phi, s_\omega, \delta$ and ρ are taken the same as in Fig. 2(a).

and

$$\sum_{k=1}^2 U_{\alpha k}^{(0)*} U_{1k}^{(0)} = \delta_{\alpha 1} - U_{\alpha 3}^{(0)*} U_{13}^{(0)}, \quad (46)$$

we obtain

$$S(x)_{\beta\alpha} = \delta_{\beta\alpha} + i T(x)_{\beta\alpha} \quad (47)$$

with

$$\begin{aligned} i T(x)_{\beta\alpha} &= -2i e^{-i \frac{\delta m_{31}^2 x}{4E}} \sin \frac{\delta m_{31}^2}{4E} U_{\beta 3}^{(0)} U_{\alpha 3}^{(0)*} \left[1 - \frac{a}{\delta m_{31}^2} \left(2 |U_{13}^{(0)}|^2 - \delta_{\alpha 1} - \delta_{\beta 1} \right) - i \frac{ax}{2E} |U_{13}^{(0)}|^2 \right] \\ &- i \frac{\delta m_{31}^2 x}{2E} \left[\frac{\delta m_{21}^2}{\delta m_{31}^2} U_{\beta 2}^{(0)} U_{\alpha 2}^{(0)*} + \right. \\ &\quad \left. \frac{a}{\delta m_{31}^2} \left\{ \delta_{\alpha 1} \delta_{\beta 1} |U_{13}^{(0)}|^2 + U_{\beta 3}^{(0)} U_{\alpha 3}^{(0)*} \left(2 |U_{13}^{(0)}|^2 - \delta_{\alpha 3} - \delta_{\beta 3} \right) \right\} \right]. \end{aligned} \quad (48)$$

We then obtain the oscillation probability in the lowest order approximation as

$$\begin{aligned} P(\nu_\alpha \rightarrow \nu_\beta; L) &= |S(L)_{\beta\alpha}|^2 \\ &= \delta_{\beta\alpha} \left[1 - 4 |U_{\alpha 3}^{(0)}|^2 \sin^2 \frac{\delta m_{31}^2 L}{4E} \left\{ 1 - 2 \frac{a}{\delta m_{31}^2} \left(|U_{13}^{(0)}|^2 - \delta_{\alpha 1} \right) \right\} \right. \\ &\quad \left. - 2 \frac{aL}{2E} \sin \frac{\delta m_{31}^2 L}{2E} |U_{\alpha 3}^{(0)}|^2 |U_{13}^{(0)}|^2 \right] \\ &+ 4 |U_{\beta 3}^{(0)}|^2 |U_{\alpha 3}^{(0)}|^2 \sin^2 \frac{\delta m_{31}^2 L}{4E} \left\{ 1 - 4 \frac{a}{\delta m_{31}^2} |U_{13}^{(0)}|^2 + 2 \frac{a}{\delta m_{31}^2} (\delta_{\alpha 1} + \delta_{\beta 1}) \right\} \\ &+ 2 \frac{\delta m_{31}^2 L}{2E} \sin \frac{\delta m_{31}^2 L}{2E} \left[\frac{\delta m_{21}^2}{\delta m_{31}^2} \text{Re} \left(U_{\beta 3}^{(0)*} U_{\beta 2}^{(0)} U_{\alpha 3}^{(0)} U_{\alpha 2}^{(0)*} \right) \right. \\ &\quad \left. + \frac{a}{\delta m_{31}^2} \left\{ \delta_{\alpha 1} \delta_{\beta 1} |U_{13}^{(0)}|^2 + |U_{\alpha 3}^{(0)}|^2 |U_{\beta 3}^{(0)}|^2 \left(2 |U_{13}^{(0)}|^2 - \delta_{\alpha 1} - \delta_{\beta 1} \right) \right\} \right] \\ &- 4 \frac{\delta m_{21}^2 L}{2E} \sin^2 \frac{\delta m_{31}^2 L}{4E} \text{Im} \left(U_{\beta 3}^{(0)*} U_{\beta 2}^{(0)} U_{\alpha 3}^{(0)} U_{\alpha 2}^{(0)*} \right). \end{aligned} \quad (49)$$

Substituting eq.(2) in eq.(49) we finally obtain eq.(22) \sim eq.(24).

Figure 5 shows how well this approximation works for KEK/Super-Kamiokande experiment and also for Minos experiment with the same masses, mixing angles and CP violating phase as in Fig. 2(a). Our approximation requires (see eq.(20))

$$\frac{aL}{2E} = 0.420 \left(\frac{L}{730 \text{ km}} \right) \left(\frac{\rho}{3 \text{ g cm}^{-3}} \right) \ll 1 \quad (50)$$

and

$$\frac{\delta m_{21}^2 L}{2E} = 0.185 \frac{(\delta m_{21}^2 / 10^{-4} \text{ eV}^2)(L / 730 \text{ km})}{E / \text{GeV}} \ll 1, \quad (51)$$

which is marginally satisfied for $L = 730 \text{ km}$. We see that even in this case eq.(49) gives good approximation.

References

- [1] GALLEX Collaboration, P. Anselmann *et al.*, Phys. Lett. B **357**, 237 (1995).
- [2] SAGE Collaboration, J. N. Abdurashitov *et al.*, Phys. Lett. B **328**, 234 (1994).
- [3] Kamiokande Collaboration, Y. Suzuki, Nucl. Phys. B (Proc. Suppl.) **38**,54 (1995).
- [4] Homestake Collaboration, B. T. Cleveland *et al.*, Nucl. Phys. B (Proc. Suppl.) **38**, 47 (1995).
- [5] Kamiokande Collaboration, K.S. Hirata *et al.*, Phys. Lett. B **205**, 416 (1988); *ibid.* B **280**, 146 (1992) ; Y. Fukuda *et al.*, Phys. Lett. B **335**, 237 (1994).
- [6] IMB Collaboration, D. Casper *et al.*, Phys. Rev. Lett. **66**, 2561 (1991); R. Becker-Szendy *et al.*, Phys. Rev. D **46**, 3720 (1992).
- [7] SOUDAN2 Collaboration, T. Kafka, Nucl. Phys. B (Proc. Suppl.) **35**, 427 (1994); M. C. Goodman, *ibid.* **38**, 337 (1995); W. W. M. Allison *et al.*, Phys. Lett. B **391**, 491 (1997).
- [8] NUSEX Collaboration, M. Aglietta *et al.*, Europhys. Lett. **8**, 611(1989); *ibid.* **15**, 559 (1991).
- [9] Fréjus Collaboration, K. Daum *et al.*, Z. Phys. C **66**, 417 (1995).
- [10] G. L. Fogli, E. Lisi, D. Montanino and G.Scioscia, Preprint IASSNS-AST 96/41 (hep-ph/9607251).
- [11] G. L. Fogli, E. Lisi and D. Montanino, Phys. Rev. D **49**, 3626 (1994).
- [12] O. Yasuda, preprint TMUP-HEL-9603 (hep-ph/9602342).
- [13] K. Nishikawa, INS-Rep-924 (1992).
- [14] S. Parke, Fermilab-Conf-93/056-T (1993) (hep-ph/9304271).
- [15] M. Tanimoto, Phys. Rev. D **55**, 322 (1997); M. Tanimoto, Prog. Theor. Phys. **97**, 901 (1997).
- [16] J. Arafune and J. Sato, Phys. Rev. D **55**, 1653 (1997).
- [17] For a review, M. Fukugita and T. Yanagida, in *Physics and Astrophysics of Neutrinos*, edited by M. Fukugita and A. Suzuki (Springer-Verlag, Tokyo, 1994).
- [18] S. M. Bilenky and S. T. Petcov, Rev. Mod. Phys. **59**, 671 (1987).
- [19] S. Pakvasa, in *High Energy Physics – 1980*, Proceedings of the 20th International Conference on High Energy Physics, Madison, Wisconsin, edited by L. Durand and L. Pondrom, AIP Conf. Proc. No. 68 (AIP, New York, 1981), Vol. 2, pp. 1164.

- [20] L. -L. Chau and W. -Y. Keung, Phys. Rev. Lett. **59**, 671 (1987).
- [21] T. K. Kuo and J. Pantaleone, Phys. Lett. B **198**, 406 (1987).
- [22] S. Toshev, Phys. Lett. B **226**, 335 (1989).
- [23] V. Barger, K. Whisnant and R. J. N. Phillips, Phys. Rev. Lett. **45**, 2084 (1980).